

## REFERENCES

- Aranovich, G. L.; Donohue, M. D. (1995). A New Approach to Analysis of Multilayer Adsorption. *J. Colloid Interface Sci.* 1995, 173, 515-520.
- Bamrungket, M. (2001). Water removal from natural gas via clinoptilolite. M.S. Thesis, The Petroleum and Petrochemical College, Chulalongkorn University.
- Brosillon, S., Manero, M.H., and Foussard, J.N. (2001). Mass transfer in VOC adsorption on zeolite: Experimental and Theoretical Breakthrough curve. *Environmental Science and Technology*, 35, 3571-3575.
- Brunauer, S., Deming, L., Deming, W., Teller, E. (1940). *J. Am. Chem. Soc.*, 62, 1723.
- Butt JB & Petersen EE (1988) Activation, deactivation and poisoning of catalysts. Academic Press, Inc., New York.
- Campbell, J.M. (1992). Gas conditioning and Processing. Oklahoma: Campbell Petroleum.
- Chaikasetpaiboon, P. (2002). Experimental and mathematical modeling of a multibed gas adsorber. M.S. Thesis, The Petroleum and Petrochemical College, Chulalongkorn University.
- Deen, W.M. (1998). Analysis of Transport Phenomena. New York, Oxford University Press, Inc. 44-46.
- Gorbach, A., Stegmaier, M., and Eigenberger, G. (2003). Measurement and modeling of water vapor adsorption on zeolite 4A-equilibria and kinetics. *Adsorption*, 10, 29-46, 2004.
- Forzatti P & Lietti L (1999) Catalyst deactivation. *Catalysis Today* 52: 165-181.
- Fogler, H.S., (2002). Elements of Chemical Reaction Engineering 3<sup>rd</sup> edition. New Jersey, Prentice-Hall Inc.
- Froment GF & Bischoff KB (1990) Chemical Reactor Analysis and Design, John Wiley & Sons., New York.
- IUPAC Recommendations, Pure Appl. Chem., 1994, 57, 603.

- Kim, J., Lee, C., Kim, W., Lee, J., Kim, J., Suh, J., and Lee, J., (2003). Adsorption Equilibria of water vapor on alumina, zeolite 13X, and a zeolite X/activated carbon composite. J. Chem. Eng., 48, 137-141.
- Kim, M., Ryu, Y., and Lee, C. (2005). Adsorption equilibria of water vapor on activated carbon and DAY zeolite. J. Chem. Eng., 50, 951-955.
- Kotoh, K., Enoeda, M., Matsui, T., and Nishikawa, M. (1993). A multilayer Model for Adsorption of Water on Activated Alumina in Relation to Adsorption Potential., J. Chem. Eng. Japan., 26, 355-360.
- Lee, J.W., Oh, J.S., Shim, W.G., Kim J.H., Moon, K., and Seo G. (2003). Adsorption equilibrium of water vapor on mesoporous materials. J.Chem.Eng., 48, 1458-1462.
- Lertviriyakijskul, S. (2000). Characterization of water and hydrocarbon adsorption properties of sol-gel alumina. M.S. Thesis, The Petroleum and Petrochemical College, Chulalongkorn University.
- Moore, J. D., and Serbebezov, A. (2005). Correlation of adsorption equilibrium data for water vapor on F-200 activated alumina. Adsorption, 11, 65-75, 2005.
- Philip A. S. (1995). Handbook of Separation Techniques for Chemical Engineers 3<sup>rd</sup> Edition., McGraw-Hill., Part 3; Gas (vapor) Mixture.
- Thomas, W. J. (1998). Adsorption technology and design. A division of Reed Education and Professional Publishing Ltd.
- Uttamaroop, T. (2003). Sensitivity analysis and development of mathematical model for water breakthrough curves of a multi-layer adsorber. M.S. Thesis, The Petroleum and Petrochemical College, Chulalongkorn University.
- <http://www.uniongas.com/> accessed on 4<sup>th</sup>, April 2006.
- <http://www.zeoponix.com/zeolite.htm> accessed on 27<sup>th</sup>, Mar 2006.

## APPENDICES

### Appendix A: Crystal size data from SEM analysis

**Table A1** Crystal size data of Molecular Sieve Zeolite of size 1/8”

Crystal size range (micron) Aging condition	%quantity				Average crystal size (micron)
	0.00-0.99	1.00-1.99	2.00-2.99	3.00-3.99	
Fresh	0.96	34.62	46.15	18.27	2.312
10 batches	4.21	47.37	37.89	10.53	2.042
20 batches	8.15	48.91	40.76	2.17	1.865
30 batches	14.04	52.63	24.56	8.77	1.776
40 batches	21.70	39.62	37.74	0.94	1.531
50 batches	51.90	34.06	13.54	1.31	1.271
60 batches	50.00	35.09	12.28	2.63	1.170
70 batches	63.97	20.65	15.38	0.00	1.168
80 batches	52.91	28.64	15.05	0.00	1.134
90 batches	58.74	23.79	16.50	0.00	1.104
100 batches	56.10	25.61	13.01	0.00	1.098
120 batches	63.40	22.50	12.60	0.00	1.064

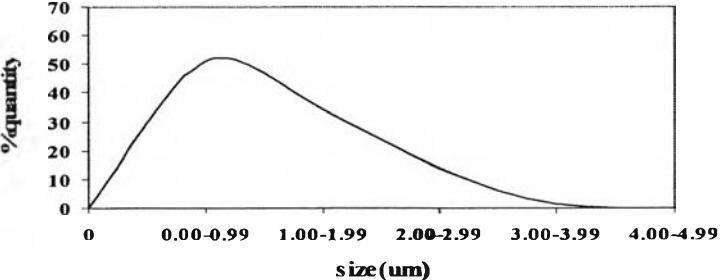
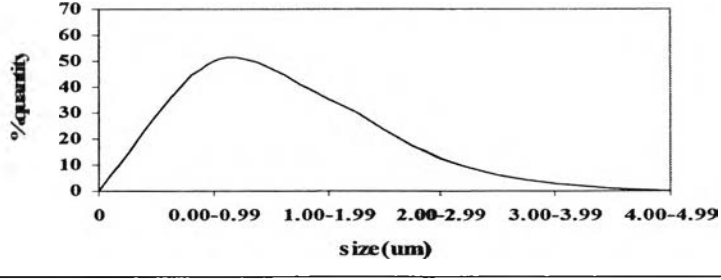
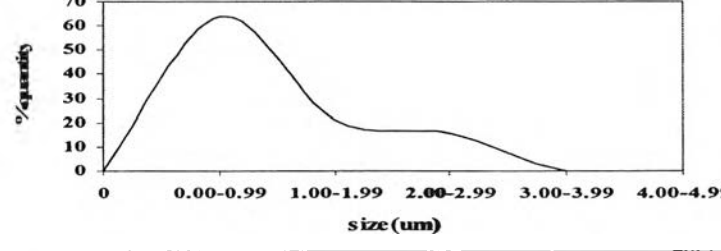
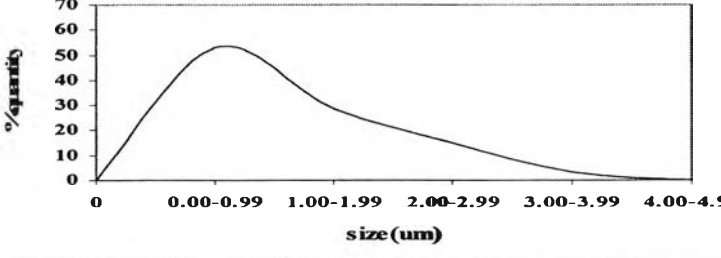
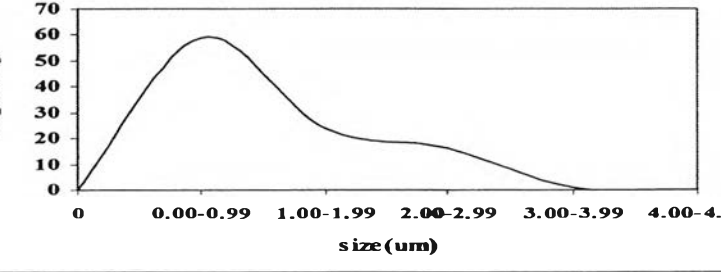
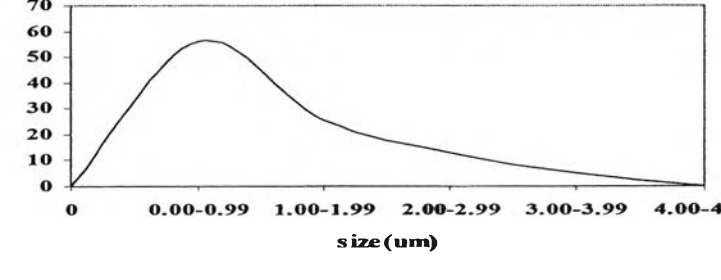
**Table A2** Crystal size data of Molecular Sieve Zeolite of size 1/16”

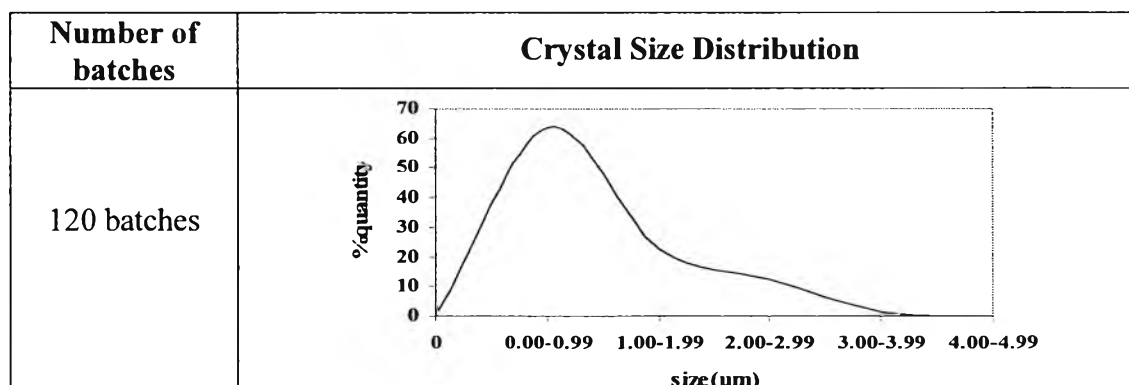
Crystal size range (micron) Aging condition	%quantity				Average crystal size (micron)
	0.00-0.99	1.00-1.99	2.00-2.99	3.00-3.99	
Fresh	12.68	33.80	33.40	19.72	2.101
10 batches	10.24	36.22	37.80	15.75	2.086
20 batches	9.21	47.37	26.32	17.11	2.008
30 batches	31.64	28.91	25.78	13.67	1.722
40 batches	34.21	30.53	22.63	12.63	1.653
50 batches	32.58	31.67	27.60	7.24	1.617
60 batches	42.97	36.88	14.45	5.70	1.328
70 batches	51.16	37.79	9.30	1.74	1.111
80 batches	54.74	32.28	11.23	1.75	1.095
90 batches	59.87	29.15	8.78	2.19	1.028
100 batches	65.38	20.94	11.54	2.14	0.999
120 batches	66.40	22.00	10.50	1.10	0.982

**Appendix B: Crystal Size Distribution of Molecular Sieve Zeolite of size 1/8”  
and 1/16”**

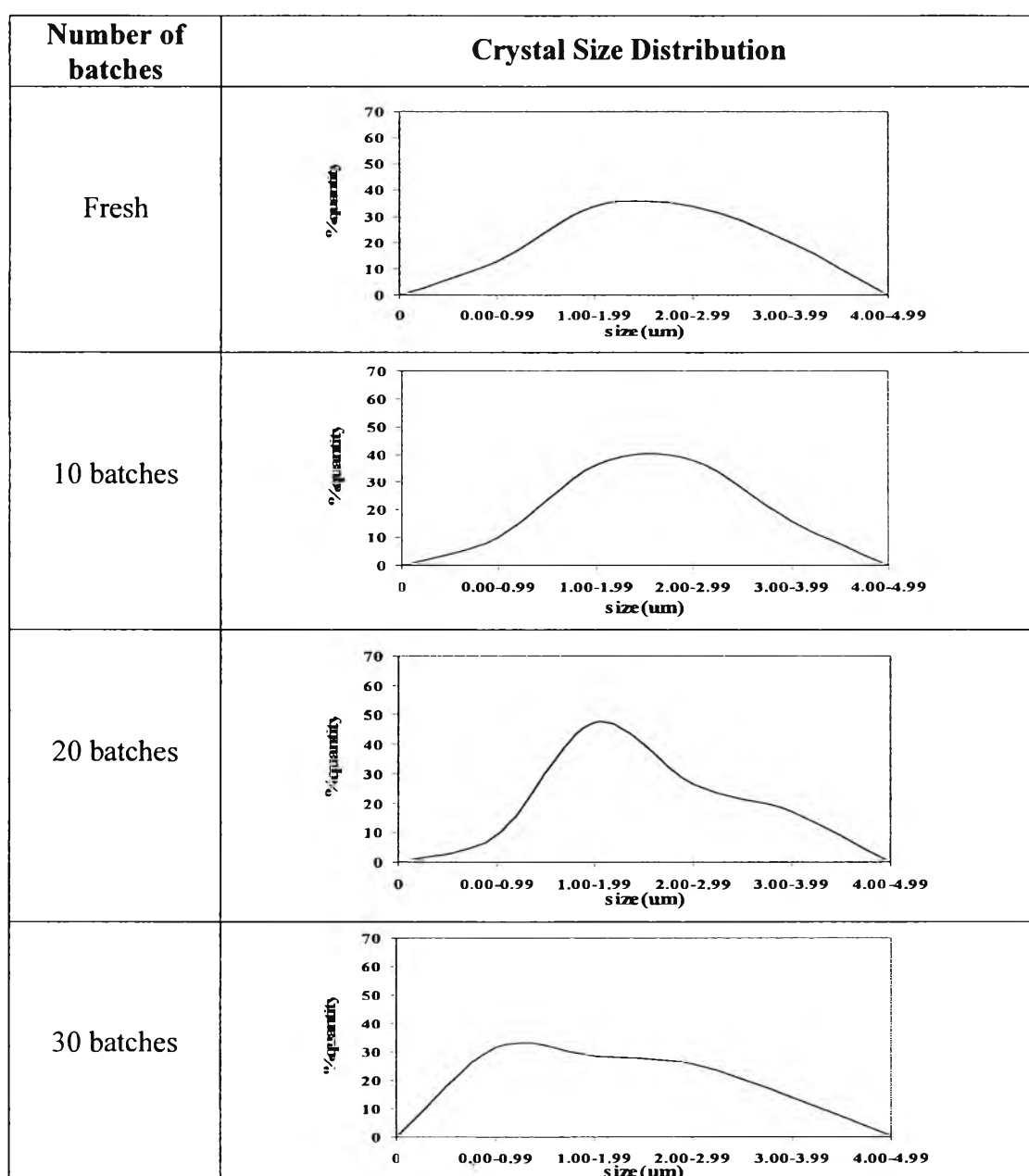
**Table B1** Crystal Size Distribution of Molecular Sieve Zeolite of size 1/8”

Number of batches	Crystal Size Distribution
Fresh	
10 batches	
20 batches	
30 batches	
40 batches	

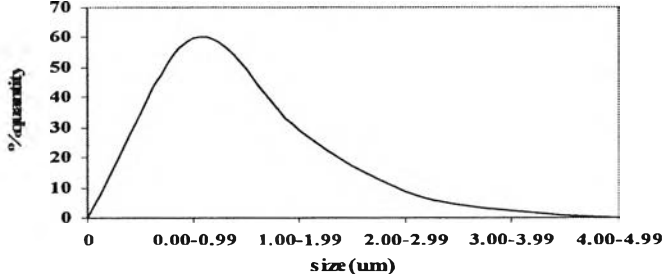
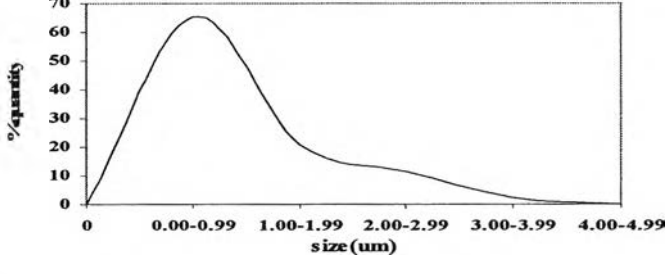
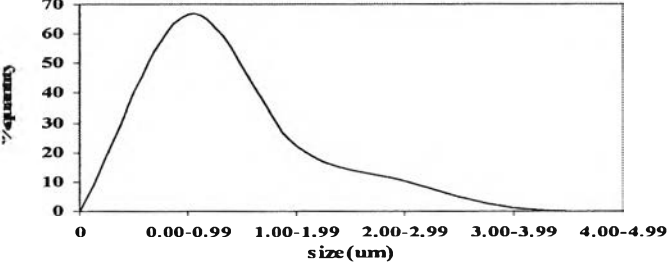
Number of batches	Crystal Size Distribution
50 batches	
60 batches	
70 batches	
80 batches	
90 batches	
100 batches	



**Table B2** Crystal Size Distribution of Molecular Sieve Zeolite of size 1/16”



Number of batches	Crystal Size Distribution
40 batches	<p>Graph showing Crystal Size Distribution for 40 batches. The y-axis represents %quantity (0 to 70) and the x-axis represents size(um) (0 to 4.00-4.99). The distribution peaks at approximately 38% quantity in the 0.00-0.99 um size range.</p>
50 batches	<p>Graph showing Crystal Size Distribution for 50 batches. The y-axis represents %quantity (0 to 70) and the x-axis represents size(um) (0 to 4.00-4.99). The distribution peaks at approximately 35% quantity in the 0.00-0.99 um size range.</p>
60 batches	<p>Graph showing Crystal Size Distribution for 60 batches. The y-axis represents %quantity (0 to 70) and the x-axis represents size(um) (0 to 4.00-4.99). The distribution peaks at approximately 45% quantity in the 0.00-0.99 um size range.</p>
70 batches	<p>Graph showing Crystal Size Distribution for 70 batches. The y-axis represents %quantity (0 to 70) and the x-axis represents size(um) (0 to 4.00-4.99). The distribution peaks at approximately 52% quantity in the 0.00-0.99 um size range.</p>
80 batches	<p>Graph showing Crystal Size Distribution for 80 batches. The y-axis represents %quantity (0 to 70) and the x-axis represents size(um) (0 to 4.00-4.99). The distribution peaks at approximately 55% quantity in the 0.00-0.99 um size range.</p>

Number of batches	Crystal Size Distribution														
90 batches	 <p>A line graph showing the crystal size distribution for 90 batches. The y-axis is labeled '% quantity' and ranges from 0 to 70. The x-axis is labeled 'size (um)' and has categories: 0, 0.00-0.99, 1.00-1.99, 2.00-2.99, 3.00-3.99, and 4.00-4.99. The curve starts at (0,0), rises to a peak of approximately 60% in the 0.00-0.99 um range, and then gradually declines to near 0% by the 4.00-4.99 um range.</p> <table border="1"><thead><tr><th>size (um)</th><th>% quantity</th></tr></thead><tbody><tr><td>0</td><td>0</td></tr><tr><td>0.00-0.99</td><td>60</td></tr><tr><td>1.00-1.99</td><td>35</td></tr><tr><td>2.00-2.99</td><td>15</td></tr><tr><td>3.00-3.99</td><td>5</td></tr><tr><td>4.00-4.99</td><td>2</td></tr></tbody></table>	size (um)	% quantity	0	0	0.00-0.99	60	1.00-1.99	35	2.00-2.99	15	3.00-3.99	5	4.00-4.99	2
size (um)	% quantity														
0	0														
0.00-0.99	60														
1.00-1.99	35														
2.00-2.99	15														
3.00-3.99	5														
4.00-4.99	2														
100 batches	 <p>A line graph showing the crystal size distribution for 100 batches. The y-axis is labeled '% quantity' and ranges from 0 to 70. The x-axis is labeled 'size (um)' and has categories: 0, 0.00-0.99, 1.00-1.99, 2.00-2.99, 3.00-3.99, and 4.00-4.99. The curve starts at (0,0), rises to a peak of approximately 65% in the 0.00-0.99 um range, and then gradually declines to near 0% by the 4.00-4.99 um range.</p> <table border="1"><thead><tr><th>size (um)</th><th>% quantity</th></tr></thead><tbody><tr><td>0</td><td>0</td></tr><tr><td>0.00-0.99</td><td>65</td></tr><tr><td>1.00-1.99</td><td>30</td></tr><tr><td>2.00-2.99</td><td>15</td></tr><tr><td>3.00-3.99</td><td>5</td></tr><tr><td>4.00-4.99</td><td>2</td></tr></tbody></table>	size (um)	% quantity	0	0	0.00-0.99	65	1.00-1.99	30	2.00-2.99	15	3.00-3.99	5	4.00-4.99	2
size (um)	% quantity														
0	0														
0.00-0.99	65														
1.00-1.99	30														
2.00-2.99	15														
3.00-3.99	5														
4.00-4.99	2														
120 batches	 <p>A line graph showing the crystal size distribution for 120 batches. The y-axis is labeled '% quantity' and ranges from 0 to 70. The x-axis is labeled 'size (um)' and has categories: 0, 0.00-0.99, 1.00-1.99, 2.00-2.99, 3.00-3.99, and 4.00-4.99. The curve starts at (0,0), rises to a peak of approximately 68% in the 0.00-0.99 um range, and then gradually declines to near 0% by the 4.00-4.99 um range.</p> <table border="1"><thead><tr><th>size (um)</th><th>% quantity</th></tr></thead><tbody><tr><td>0</td><td>0</td></tr><tr><td>0.00-0.99</td><td>68</td></tr><tr><td>1.00-1.99</td><td>25</td></tr><tr><td>2.00-2.99</td><td>15</td></tr><tr><td>3.00-3.99</td><td>5</td></tr><tr><td>4.00-4.99</td><td>2</td></tr></tbody></table>	size (um)	% quantity	0	0	0.00-0.99	68	1.00-1.99	25	2.00-2.99	15	3.00-3.99	5	4.00-4.99	2
size (um)	% quantity														
0	0														
0.00-0.99	68														
1.00-1.99	25														
2.00-2.99	15														
3.00-3.99	5														
4.00-4.99	2														



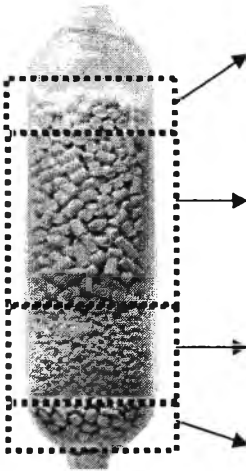
### Appendix C: Conditions for Adsorption experiments

**Table C** Conditions for Adsorption Experiments

<b>Parameters</b>	<b>Value</b>
Weight of adsorbent packed in adsorber	about 5 g
Operating pressure (const.)	1 atm
Operating temperature (isothermal)	25°C
Humidity of natural gas feed	5-75%RH
Natural gas feed flow rate	
Activated alumina	115.1 ml/min
Molsiv (1/8")	125.8 ml/min
Molsiv (1/16")	138.8 ml/min
Contact time(based on feed flow rate)	
Activated alumina	11.83 sec
Molsiv (1/8")	10.82 sec
Molsiv (1/16")	9.81 sec
Bed volume	24.3 ml

### Appendix D: Conditions for breakthrough curve experiments

**Table D** Multi-layer adsorber

Adsorber layout	Adsorbent type	Height (cm)	Actual volume ratio* (%)
 <p>Bed volume: 75ml</p>	Activated alumina	0.3	3.41
	MolSiv Zeolite type 4A size 1/8"	5.6	63.64
	MolSiv Zeolite type 4A size 1/16"	2.9	32.95
	Ceramic ball	Inert material used as an adsorbent support	

\*PTT Public Co.Ltd.

## Appendix E: Parameters Applied in the Mathematical Model

### E.1 Parameters Applied in the Mathematical Model

**Table E1** Parameters applied in the mathematical model

Parameter	alumina	1/8" 4A Molsiv	1/16" 4A Molsiv
Bed void fraction*, $\varepsilon$	0.37	0.35	0.34
Axial dispersion coefficient**, $D_L$	0.02824	0.027733	0.027170
Bulk density***, (g/cm <sup>3</sup> )	0.73743	0.66529	0.66529

\* Appendix F

\*\* Appendix E.3

\*\*\* UOP information

### E.2 Interstitial velocity

Since the interstitial velocity can be calculated from the correlation,  $v_i = v_s / \varepsilon$ , so the superficial velocity and bed void fraction are needed.

- Superficial velocity

$$v_s = \frac{Q}{A}$$

Where,  $Q = 457.78$  ml/min

$A =$  cross sectional area of adsorber = 8.55 cm

So,  $v_s = 53.52$  ml/min

- Interstitial velocity

$$v_i = \frac{v_s}{\varepsilon}$$

	$\varepsilon$	$v_i$ (ml/min)	contact time(sec)
alumina	0.37	144.65	0.964
molsiv(1/8")	0.35	152.91	18.73
molsiv(1/16")	0.34	157.41	9.42
		all bed	9.83

### E.3 Dispersion Coefficient

- Molecular diffusion coefficient,  $D_m$  is calculated from Chapman-Enskog equation.

$$D_m = \frac{0.0018583T^{3/2}(1/M_A + 1/M_B)^{1/2}}{P * \sigma_{AB}^2 \Omega_{AB}}$$

Where,  $M_A$  = average molecular weight of bulk species (natural gas) = 20.59

$M_B$  = molecular weight of adsorbate species (water) = 18

$\sigma_{AB}$  = collision diameter from Lennard-Jones potential = 3.29352 °A

$\Omega_{AB}$  = collision integral = 1.60089

$P$  = total pressure in atmospheres = 1 atm

$T$  = temperature = 298 K

### Appendix F: Bed void fraction of each adsorbent

The bed void fraction of the adsorbents used in the packed bed adsorber can be obtained from Figure F1.

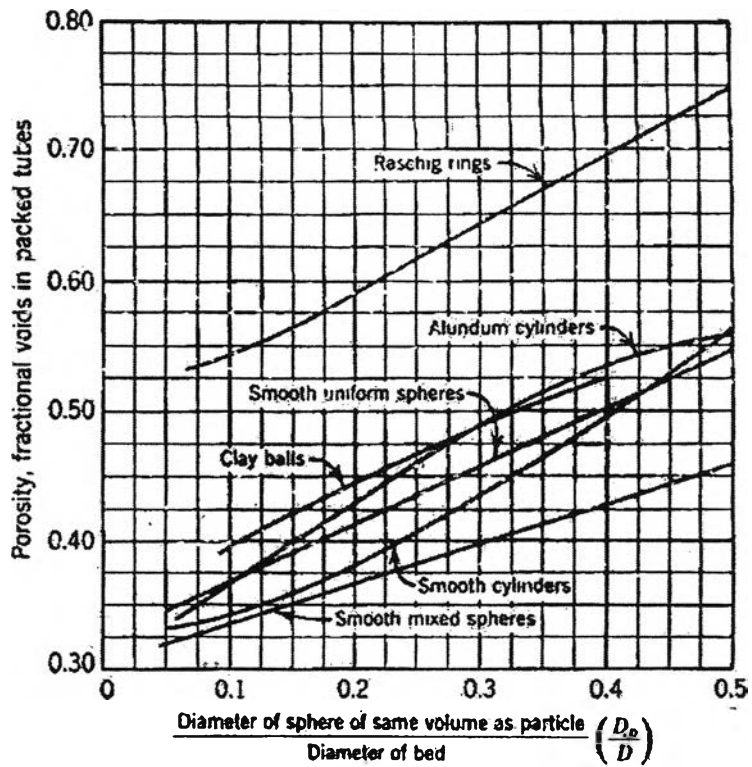


**Figure F** The porosity as a function of the ratio of particle diameter to bed diameter (Leva, 1947).

### Appendix G: Sensitivity of Overall Mass Transfer Coefficient (k) to the Shape of the Breakthrough Curve

Uttamaroop (2003) indicated the increase of overall mass transfer coefficient resulted in steeper breakthrough curve, and then the  $k$  value of about  $8.5 \times 10^{-5} \text{ s}^{-1}$  was suggested. But in this work, the result obtained from the slope of theoretical breakthrough curve using  $k = 8.5 \times 10^{-5} \text{ s}^{-1}$  was quite different from the experimental one as shown in Figure G1. So, the breakthrough curve from using the  $k$  value of about  $5.0 \times 10^{-5} \text{ s}^{-1}$  was examined, and it was found the breakthrough pattern was similar to the experimental one. But the breakthrough time predicted from the model of  $k = 8.5 \times 10^{-5} \text{ s}^{-1}$  was more precise, with 6.47% error from the experiment. The difference of errors is shown in Table G1. Thus, the breakthrough curve using  $k = 8.5 \times 10^{-5} \text{ s}^{-1}$  was employed for good agreement with the experimental data under identical conditions.

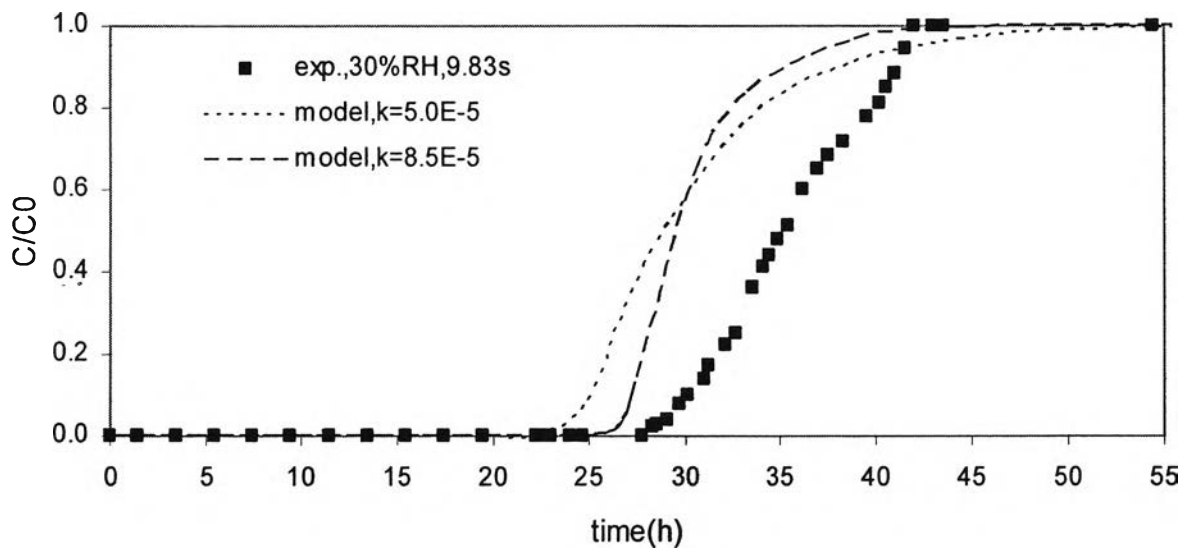


**Figure G** Comparison between the experimental and theoretical breakthrough curves with the influence of the overall mass transfer coefficient at the contact time of 9.83 sec and the feed humidity of 30%RH.

**Table G** Comparison of breakthrough time predicted from several  $k$  value

<b>k value</b>	<b>Theoretical breakthrough time(h)</b>	<b>% Error</b>
5.0 E-05	25	10.07
8.5 E-05	26	6.47

## **Appendix H: Effect of the Bed Voidage on the Breakthrough Time of Deactivated Adsorbents**

The equilibrium adsorption isotherm equations of deactivated adsorbents were applied in the mathematical model to predict the breakthrough profile at the same conditions. From the model, the breakthrough occurs at around 19 hours, resulting in about 20.83 % error from the experiment. Therefore, another parameter related to the adsorbent deactivation inside the packed bed, which is bed voidage, was studied.

The void fraction of deactivated adsorbents were corrected based on the sensitivity analysis of Uttamaroop (2003), which suggested that the theoretical breakthrough curve shifted to the longer time when the bed void fraction decreased. This suggestion was supported with the result from the adsorbents characterization part which when the molecular sieve zeolite were deactivated, the pellets were destroyed, and their size were decreased. Thus, the corrected void fractions for both molecular sieves were applied in the model and gave the good agreement with the experimental data. New void fractions were measured and calculated using data from Appendix F and shown in Table H1. The new breakthrough time was around 22 hours and gave about 8.3% error.

**Table H** The bed void fraction provided in the theoretical breakthrough model for 88.3% deactivated alumina, 15.13% deactivated 1/8” molsiv, and 14.10% deactivated molsiv at the contact time of 9.83 sec and the feed humidity of 30%RH

<b>Adsorbent</b>	<b>Void fraction</b>	<b>Corrected void fraction</b>
alumina	0.37	0.37
1/8” molsiv	0.35	0.30
1/16” molsiv	0.34	0.29

In addition, another parameter that could affect the theoretical breakthrough curve when the void fraction changes is the axial dispersion coefficient because this parameter obtained from calculation by taking into account the void

fraction in calculation. But from sensitivity analysis by Uttamaroop (2003), it was found the theoretical breakthrough curve was not sensitive to the change of axial dispersion coefficient. So, the effect of this parameter was not studied in this work.

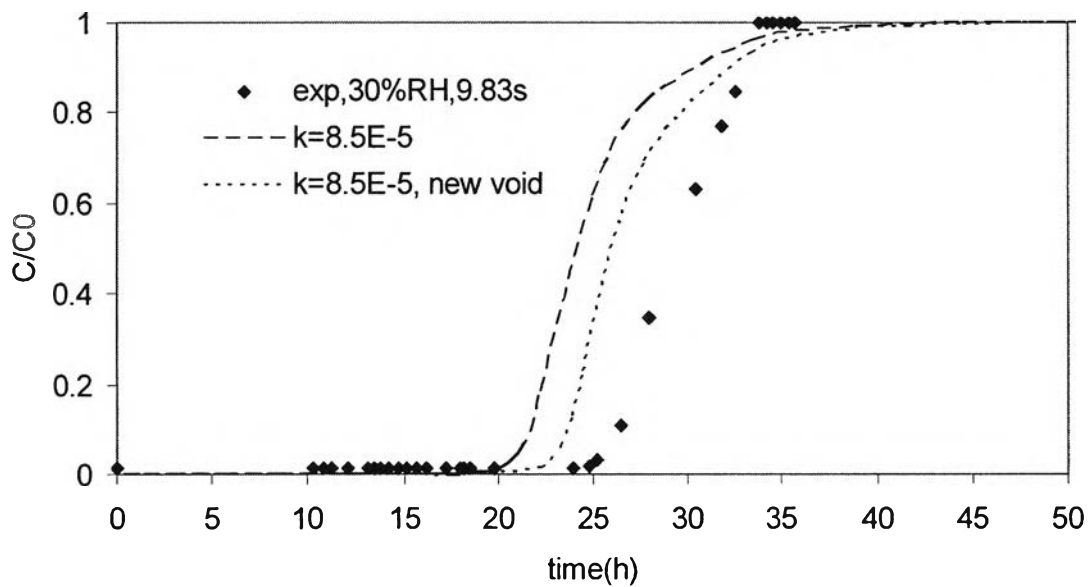


**Figure H** Comparison between the experimental and theoretical breakthrough curves of deactivated adsorbents at the contact time of 9.83 sec and the feed humidity of 30%RH.



### Appendix I: Hydrothermal steaming apparatus

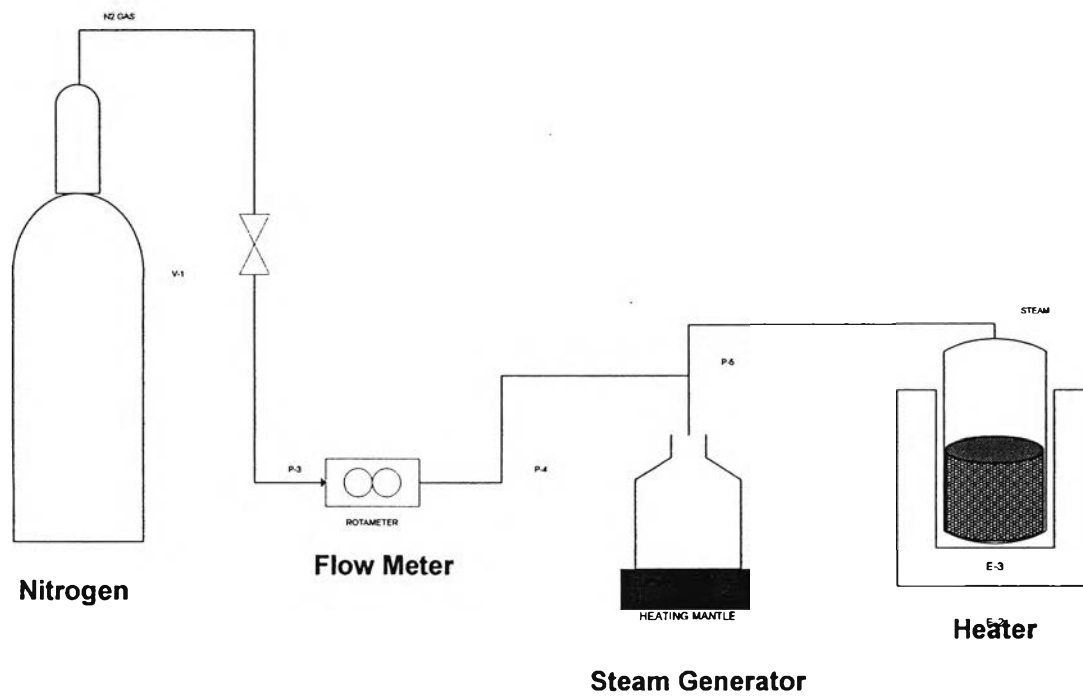


**Figure I** Hydrothermal steaming apparatus.

## Appendix J: Simulation Program

PROGRAM BREAKTHROUGH CURVE PREDICTION

```

! for the assumption of velocity is not constant

IMPLICIT NONE
DOUBLE PRECISION C0,C,q,dt,KC,Kq,time,Csat,RH
DOUBLE PRECISION v1,v,e_A,e_B,e_C
INTEGER i,j,imax,jmax,n
PARAMETER(imax=90,jmax=5000)
DIMENSION C(imax,jmax),q(imax,jmax),v(imax,jmax)
DIMENSION KC(4,imax,jmax),Kq(4,imax,jmax)

c .....INITIAL CONDITION.....
dt = 0.008
time=0
j=1                                !at time = 0
RH = 30
Csat=1.2794E-03
C0 = RH*Csat/100                    !inlet concentration (mol/l)
C(1,j)=C0
v1= 0.8920833                       ! Superficial velocity
e_A=0.37
e_B=0.35
e_C=0.34
v(1,j)=v1/e_A

OPEN(5,file='velocity.dat')

DO i=2,imax

    C(i,j)=0
    q(i,j)=0

END DO

OPEN(1,file='data1.dat')

DO i=1,imax
    WRITE(1,101)time,i,j,C(i,j),q(i,j),v(i,j)
END DO

    Call RK4(j,C,q,v,imax,jmax,KC,Kq,dt)

GOTO 20

10 OPEN(2,FILE='DATA2.DAT')

DO i=2,imax

    READ(2,102)time,C(i,1),q(i,1),v(i,1),(KC(n,i,1),n=1,4)
1    ,(Kq(n,i,1),n=1,4)

END DO

20 DO j=2,jmax

```

```

DO i=2,imax
    v(1,j)=v1/e_A
    C(1,j)=C0
    C(i,j)=C(i,j-1)+(dt/6)*(KC(1,i,j-1)+2*KC(2,i,j-1)
1      +2*KC(3,i,j-1)+KC(4,i,j-1))
    q(i,j)=q(i,j-1)+(dt/6)*(Kq(1,i,j-1)+2*Kq(2,i,j-1)
1      +2*Kq(3,i,j-1)+Kq(4,i,j-1))
END DO
Call    RK4(j,C,q,v,imax,jmax,KC,Kq,dt)
END DO
C      .....The Results.....

DO j=1,jmax
    time=time+dt      !sec
END DO

CLOSE(2)
OPEN(2,file='data2.dat')
DO i=2,imax
    WRITE(2,102)time,C(i,jmax),q(i,jmax),v(i,jmax)
1    , (KC(n,i,jmax),n=1,4), (Kq(n,i,jmax),n=1,4)
    WRITE(5,102)time,C(i,jmax),q(i,jmax),v(i,jmax)
    OPEN(3,file='FFF_NEW_30%RH&9.83sec(vnotconst).dat')
    IF(i.EQ.imax)THEN
        WRITE(3,102)time,C(i,jmax),q(i,jmax),v(i,jmax)
    ELSE
    END IF
END DO
CLOSE(2)
c      .....Check Running Loop.....

IF(time.LT.300000) THEN
GOTO 10
ELSE
GOTO 999
END IF

C      .....Format for Input and Output Statements.....
101  FORMAT(F13.3,I3,I6,2E15.9,8E15.9)
102  FORMAT(F13.3,3E15.9,8E15.9)
999  STOP
     CLOSE(3)
     END

```

```

c *****
SUBROUTINE RK4(j,C,q,v,imax,jmax,KC,Kq,dt)

IMPLICIT NONE
DOUBLE PRECISION CC,qq,C,q,dC_dt,dq_dt,dt,KC,Kq,v
INTEGER i,j,imax,jmax
DIMENSION C(imax,jmax),q(imax,jmax),dC_dt(imax,jmax)
DIMENSION dq_dt(imax,jmax),KC(4,imax,jmax),Kq(4,imax,jmax)
DIMENSION CC(imax,jmax),qq(imax,jmax),v(imax,jmax)

c .....Define Parameter.....

DO i=1,imax

  CC(i,j)=C(i,j)
  qq(i,j)=q(i,j)

END DO

Call ODEs_EQ(j,imax,jmax,CC,qq,dC_dt,dq_dt,v)

DO i=2,imax

  KC(1,i,j)=dC_dt(i,j)
  Kq(1,i,j)=dq_dt(i,j)
  CC(i,j)=CC(i,j)+(dt/2)*KC(1,i,j)
  qq(i,j)=qq(i,j)+(dt/2)*Kq(1,i,j)

END DO

  Call ODEs_EQ(j,imax,jmax,CC,qq,dC_dt,dq_dt,v)

DO i=2,imax

  KC(2,i,j)=dC_dt(i,j)
  Kq(2,i,j)=dq_dt(i,j)

  CC(i,j)=CC(i,j)+(dt/2)*KC(2,i,j)
  qq(i,j)=qq(i,j)+(dt/2)*Kq(2,i,j)

END DO

  Call ODEs_EQ(j,imax,jmax,CC,qq,dC_dt,dq_dt,v)

DO i=2,imax

  KC(3,i,j)=dC_dt(i,j)
  Kq(3,i,j)=dq_dt(i,j)

  CC(i,j)=CC(i,j)+(dt)*KC(3,i,j)
  qq(i,j)=qq(i,j)+(dt)*Kq(3,i,j)

END DO

  Call ODEs_EQ(j,imax,jmax,CC,qq,dC_dt,dq_dt,v)

```



```

j=j
c .....Zone-A (Alumina).....

a1=1.195                ! For Freundlich-Isotherm
b1=0.8313

DO i=2,4

    qstar(i,j)=a1*(C(i,j)**b1)

    dq_dt(i,j)=k1*(qstar(i,j)-q(i,j))

    d2C_dz2(i,j)=(1/(dz**2))*(C(i+1,j)-2*C(i,j)+C(i-1,j))
    dC_dz(i,j)=(1/(2*dz))*(C(i+1,j)-C(i-1,j))

    dv_dz(i,j)=-((1-e_A)/(e_A*Ct))*dq_dt(i,j)*db_A/1.8

    v(i,j)=dz*(dv_dz(i,j))+v(i-1,j)

    dC_dt(i,j)=DL_A*d2C_dz2(i,j)-v(i,j)*dC_dz(i,j)
1    -((1-e_A)/e_A)*dq_dt(i,j)*db_A/1.8-C(i,j)*dv_dz(i,j)

END DO
c .....Zone-B (Mol Siv 1/8").....

Psat=3169904.00
b2=4.575E+09           ! For A-D Toth Model
t1=1.9707072
d1=0.1042178
qm_B=9.72              ! monolayer capacity

DO i=5,60

    P(i,j)=C(i,j)*RT*Pa

    qqm(i,j)=P(i,j)/(((b2+P(i,j)**t1)**(1/t1))
1    *(1-P(i,j)/Psat)**d1)

    qstar(i,j)=qqm(i,j)*1.8*qm_B

    C(i,j)=P(i,j)/(RT*Pa)

    dq_dt(i,j)=k1*(qstar(i,j)-q(i,j))

    d2C_dz2(i,j)=(1/(dz**2))*(C(i+1,j)-2*C(i,j)+C(i-1,j))
    dC_dz(i,j)=(1/(2*dz))*(C(i+1,j)-C(i-1,j))

    dv_dz(i,j)=-((1-e_B)/(e_B*Ct))*dq_dt(i,j)*db_B/1.8

    v(5,j)=v(5,j)*e_A/e_B

    v(i,j)=dz*(dv_dz(i,j))+v(i-1,j)

    dC_dt(i,j)=DL_B*d2C_dz2(i,j)-v(i,j)*dC_dz(i,j)
1    -((1-e_B)/e_B)*dq_dt(i,j)*db_B/1.8-C(i,j)*dv_dz(i,j)

```

```

END DO
c .....Zone-C (Mol Siv 1/16").....

b3=1.889E+14 !For A-D Toth Model
t2=2.8666471
d2=0.144046
Psat=3169904.00
qm_C=9.83 ! monolayer capacity

DO i=61,89

    P(i,j)=C(i,j)*RT*Pa

    qqm(i,j)=P(i,j)/(((b3+P(i,j)**t2)**(1/t2))
1    *(1-P(i,j)/Psat)**d2)

    qstar(i,j)=qqm(i,j)*1.8*qm_C

    C(i,j)=P(i,j)/(RT*Pa)

    dq_dt(i,j)=k1*(qstar(i,j)-q(i,j))

    d2C_dz2(i,j)=(1/(dz**2))*(C(i+1,j)-2*C(i,j)+C(i-1,j))

    dC_dz(i,j)=(1/(2*dz))*(C(i+1,j)-C(i-1,j))

    dv_dz(i,j)=-((1-e_C)/(e_C*Ct))*dq_dt(i,j)*db_C/1.8

    v(60,j)=v(60,j)*e_B/e_C

    v(i,j)=dz*(dv_dz(i,j))+v(i-1,j)

    dC_dt(i,j)=DL_C*d2C_dz2(i,j)-v(i,j)*dC_dz(i,j)
1    -((1-e_C)/e_C)*dq_dt(i,j)*db_C/1.8-C(i,j)*dv_dz(i,j)

END DO

i=imax
qstar(imax,j)=qstar(imax-1,j)

dq_dt(imax,j)=dq_dt(imax-1,j)

d2C_dz2(imax,j)=0

dC_dz(imax,j)=0

dC_dt(imax,j)=dC_dt(imax-1,j)

dv_dz(imax,j)=dv_dz(imax-1,j)

v(imax,j)=v(imax-1,j)

Return

End

```

## CURRICULUM VITAE

**Name:** Ms. Wanaporn Khaikham

**Date of Birth:** November 15, 1982

**Nationality:** Thai

**University Education:**

2000-2004 Bachelor Degree of Science (Industrial Chemistry), Faculty of Science, Chiangmai University, Chiangmai, Thailand, with 2<sup>nd</sup> honor.